Per-pixel Classification of High Spatial Resolution Satellite Imagery for Urban Land-cover Mapping

David Barry Hester, Halil I. Cakir, Stacy A.C. Nelson, and Siamak Khorram

Abstract

Commercial high spatial resolution satellite data now provide a synoptic and consistent source of digital imagery with detail comparable to that of aerial photography. In the work described here, per-pixel classification, image fusion, and GIS-based map refinement techniques were tailored to pan-sharpened 0.61 m QuickBird imagery to develop a six-category urban land-cover map with 89.3 percent overall accuracy (κ = 0.87). The study area was a rapidly developing 71.5 km^2 part of suburban Raleigh, North Carolina, U.S.A., within the Neuse River basin. "Edge pixels" were a source of classification error as was spectral overlap between bare soil and impervious surfaces and among vegetated cover types. Shadows were not a significant source of classification error. These findings demonstrate that conventional spectral-based classification methods can be used to generate highly accurate maps of urban landscapes using high spatial resolution imagery.

Introduction

The recent emergence of high spatial resolution satellite image sensors has introduced an exciting new set of possibilities for analyzing imperviousness and other land-cover types at fine levels of detail. Commercial satellites including GeoEye's Ikonos (1 m panchromatic ground resolution; **www.geoeye.com**) and DigitalGlobe's QuickBird (0.61 m panchromatic ground resolution; **www.digitalglobe.com**) acquire imagery at a spatial resolution previously possible to aerial platforms alone. Continuing this trend, the planned 2008 launch of the GeoEye-1 sensor will herald even higher spatial resolution (0.41 m panchromatic ground resolution; **www.geoeye.com**). This level of spatial quality builds on advantages satellite imagery has conventionally had over aerial-derived imagery, including its capacity for synoptic coverage and its inherently digital format (Barr and Barnsley, 2000; Cablk and Minor, 2003). Such high spatial resolution space-derived imagery has already been used successfully in a diverse array of environmental mapping efforts such as earthquake damage assessment (Miura and Midorikawa, 2006), orchard and vineyard identification (Warner and Steinmaus, 2005), rain forest tree mortality inventory (Clark *et al.*, 2004), and coral reef delineation (Maeder *et al.*, 2002).

Conventional per-pixel classifiers, such as the maximum likelihood and minimum distance-to-mean algorithms, are spectral-based classification methods and constitute a historically dominant approach to remote sensing-based automated land-use/land-cover (LULC) derivation (Gao *et al.*, 2004). The maximum likelihood classifier, in fact, is frequently used as a "benchmark" against which novel classification algorithms are evaluated (Song *et al.*, 2005). Such classifiers are widely available in commercial image processing software packages and enjoy widespread user familiarity. It has been suggested, however, that traditional per-pixel classification methods have limited applicability to high spatial resolution data because they cannot fully exploit its information content (Hu *et al.*, 2005). Other analysts have reported that the detail of high spatial resolution imagery has confounded conventional automated land-cover classification techniques, particularly in studies of heterogeneous urban environments. Reportedly problematic aspects have included shadows (Barr and Barnsley, 2000; Dare, 2005), high reflectance variability but limited spectral information (Carleer *et al.*, 2005), general image complexity (Hu *et al.*, 2005), and data volume (Fisher and Goetz, 2001).

Several spectral-based classification studies of high spatial resolution imagery have been more successful. Goetz *et al.* (2003) reported overall and per category accuracies of between 75 and 85 percent for supervised and unsupervised classifications of a leaf-on and leaf-off mosaic of 4 m Ikonos imagery. The researchers in that study also used decision tree classifiers that incorporated only spectral information, including band ratios, to map urban imperviousness and tree canopy with overall accuracies of 84.2 percent and 97.3 percent, respectively. Sawaya *et al.* (2003), also working with Ikonos data, adapted modeling approaches developed for Landsat TM data to accurately describe urban lake water clarity using unsupervised per-pixel classification (r^2 = 0.94) and developed regression equations between Ikonos-derived normalized difference vegetation index (NDVI) values and sample area percent imperviousness. These equations were used to estimate percent impervious surface with a reference-data correlation of 0.98.

Thomas *et al.* (2003) concluded that their pixel-based approach to urban impervious surface mapping using high spatial resolution imagery had only moderate success due to

Department of Forestry and Environmental Resources, North Carolina State University, Campus Box 7106, Raleigh, NC 27695 (halil_cakir@ncsu.edu).

Photogrammetric Engineering & Remote Sensing
Vol. 74, No. 4, April 2008, pp. 463–471.

0099-1112/08/7404–0463/$3.00/0

the limited spectral content of that data. That study classified land-cover in an urban desert ecosystem using 8-bit aerial scanner imagery. Notably, several high spatial resolution satellite image sensors, including Ikonos, QuickBird, and GeoEye's future GeoEye-1 satellite, are designed to record reflectance data in 11-bit radiometric depth. The result is imagery with a special blend of modest spectral resolution but rich reflectance storage capacity. This is particularly important in light of innovative data fusion methods that allow analysts to merge multispectral content with its higher spatial-resolution panchromatic corollary (Svab and Osti, 2006).

Other data fusion varieties may also be useful to high spatial resolution image classification. The integration of ancillary GIS data with per-pixel classification has long been a successful land-cover derivation technique with a variety of medium- and low-resolution image types (Foody, 1995; Ludwig *et al.*, 2003; Lunetta *et al.*, 2003), but, as of yet, its applicability to high-resolution data has only been cursorily examined (Sawaya *et al.*, 2003; Thomas *et al.*, 2003). This is despite the inherent suitability of such imagery to these techniques, the efficacy of which depends on sufficient geographic alignment (Cablk and Minor, 2003).

The utility of per-pixel classification in analyzing high spatial resolution satellite data is an important research direction because pixel-based classification enjoys widespread familiarity and software accessibility due to its historical prominence. This paper describes a per-pixel classification approach used to accurately generate an urban land-cover map using fused sub-meter high spatial resolution satellite imagery, and the incorporated methods are readily available in standard remote sensing and GIS analysis packages. In order to provide a more robust account of the applicability of these conventional methods to one promising use of high spatial resolution imagery in urban areas, the accuracies of output impervious surface maps were analyzed using both point- and area-based metrics.

Study Area

The study area incorporates 71.5 km^2 of adjacent drainage catchments and is located in the northeast part of Raleigh, North Carolina. This area is composed of primarily urban and suburban land uses interspersed with large forested clusters and includes part of a major transportation corridor, US-1 (Figure 1). Raleigh is a part of Wake County and the Neuse River watershed, the third largest river basin in the state of North Carolina. This basin drains all or part of twenty-three counties into the Albemarle-Pamlico Sound; its ecological integrity has been the subject of numerous studies in recent decades (Burkholder *et al.*, 1992; McMahon and Lloyd, 1995; Paerl *et al.*, 1998).

Based on population estimates encompassing 01 April 2000 to 01 July 2005, the U.S. Census Bureau recently described Wake County as one of the 26 counties had population gains of more than 100,000 in United States (2006). This rapid level of urban and population expansion has become a major concern of state, federal, and local agencies seeking to safeguard water quality in the Neuse River watershed. Indeed, both of the major streams within the study area, Marsh Creek and Perry Creek, have been included on North Carolina's federally-mandated Clean Water Act, Section 303 (d), Impaired Waters List every year since its inception. Each time, the state has cited "urban runoff/storm sewers" as the likely cause of impairment (North Carolina Division of Water Quality, 2004). The present study is part of a larger effort to describe the rapid land-cover change occurring in the Raleigh area and to evaluate its potential impacts on water quality.

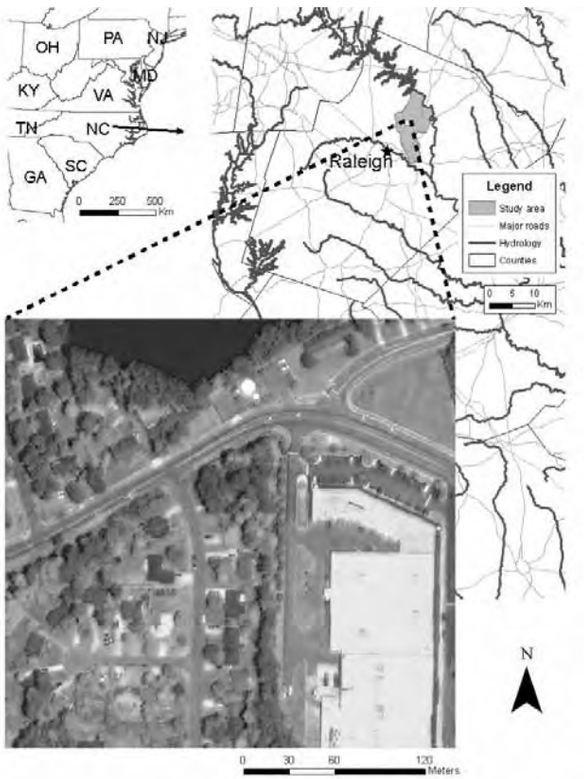

Figure 1. Raleigh, North Carolina study area depicted regionally and locally. Study area is shown on local map in shaded gray, and inset figure is a large-scale QuickBird image subset. A color version of this figure is available at the ASPRS website: **www.asprs.org**.

Data and Image Preprocessing

For this study, multispectral and panchromatic QuickBird imagery was obtained from DigitalGlobe's image archives. The image was collected on 01 June 2002 under clear atmospheric conditions at 1601 local time and at 10.1° off-nadir. The taskable QuickBird sensor is capable of collecting imagery up to 30.0° off-nadir. At the time of data collection, the sun azimuth was 126.5° and the sun elevation was 69.4°, while the satellite's azimuth and elevation metrics were 136.4° and 79.0°, respectively.

At nadir, the QuickBird sensor collects data in three visible channels (450 to 520 nm, 520 to 600 nm, and 630 to 690 nm) and one near-infrared channel (760 to 900 nm) at 2.44 m spatial resolution. Its panchromatic (445 to 900 nm) sensor images scenes at 0.61 m spatial resolution. All data are recorded in 11-bit radiometric storage depth. Using image fusion algorithms, multispectral satellite imagery can be spatially sharpened with panchromatic imagery. Data fusion, in this sense, is the combination of the two image types that results in one image with panchromatic ground resolution and multispectral spectral resolution (Pohl and van Genderen, 1998). The Cakir-Khorram algorithm used in this study (Cakir and Khorram, 2004) achieves this combined resolution while preserving spectral integrity better than conventional image fusion algorithms, such as principal components analysis and intensity-hue-saturation fusion. The resulting pan-sharpened multispectral image has a ground resolution of 0.61 m.

In order to georeference the image, 32 ground control points were field-collected throughout the study area using differentially-corrected Trimble Pro XR Global Positioning System (GPS) data. These points, recorded with a sub-meter accuracy margin of error, were then used to resolve geometric distortion within the image using a first-order polynomial correction. This algorithm was applied systemically to the image and achieved a root mean square error (RMSE) of 1.6 m. This RMSE was considered acceptable given the high spatial resolution of the imagery and the one-meter error limitation of the DGPS. The imagery was then projected to North Carolina State Plane, NAD83 datum, in meters, to match existing ancillary GIS data including roads, hydrography, and Raleigh municipal zoning layers. All image processing was performed in Leica Geosystem's ERDAS Imagine® 8.7; all GIS analyses were performed in ArcGIS® 9.0.

Per-pixel Land-cover Classification

A hybrid per-pixel classification approach was developed for urban land-cover mapping in this analysis. Such an approach acknowledges the benefits of both supervised and unsupervised classification (Kelly *et al.*, 2004). Six categories of land-cover, including impervious surface, were selected for mapping within the study area (Table 1). These categories were chosen based on their applicability to water quality analysis as well as their relevance to high spatial resolution image analysis. For example, discrete impervious land-cover features in this imagery include sidewalks, roads, and buildings. Thus, in contrast to many analyses of coarser-resolution data, it is not necessary to indirectly represent impervious features by mapping aggregate classes of land-cover which specify, for example, a broad range of impervious surface coverage within a land-use class. This approach is often adopted in light of sensor resolution limitations, although innovative recent work has sought to estimate impervious surface area at sub-pixel levels using medium-resolution data such as that of Landsat (Yang *et al.*, 2003; Jennings *et al.*, 2004). The possibility of directly mapping land-cover extent, such as imperviousness, is a primary allure of using high spatial resolution imagery (Jensen and Cowen, 1999; Barr and Barnsley, 2000).

The hybrid classification process employed for the present study is summarized in Figure 2. As an initial step in this process, a supervised classification was performed using the maximum likelihood algorithm and 25 classes. A total of 138 training sites were digitized throughout the study area following well-established manual training site generation protocols (Jensen, 2005). These training sites included at least five examples of each representative feature type within the six broad land-cover categories described in Table 1. Furthermore, illuminated and shaded versions of relevant land-cover feature types were represented by separate training site groups. For example, the impervious category was represented by five homogeneous training sites for the following feature types: concrete-like, concrete-like (shaded), asphalt-like, asphalt-like (shaded), green roofs, white roofs, red roofs, brown roofs, red recreational court surfaces, and green recreational court surfaces. This training site assemblage was taken to be exhaustive only with respect to the dominant land-cover feature types within a given category. Certain features with highly variable reflectance, such as vehicles, or features with isolated representation, such as railroad tracks, were not included in the training site scheme, a limitation addressed by the unsupervised element of this hybrid classification approach.

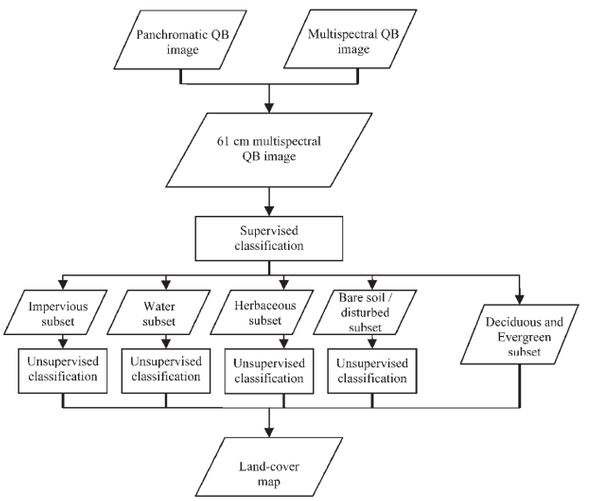

Figure 2. Flow chart summarizing hybrid per-pixel classification method.

After the output from the supervised classification was aggregated into the six classes of land-cover interest, categories that evidenced classification confusion based on visual inspection were subset. Within each of these image subsets, an unsupervised classification was performed using 25 classes, ISODATA (Iterative Self-Organizing Data Analysis Technique) clustering, principal axis means computing, 25 maximum iterations, and a 95 percent convergence threshold. Ultimately, this second classification step was carried out for each of the initial supervised classification outputs except the two categories of woody vegetation: evergreen and deciduous. After the unsupervised classifications were completed and pixels were re-categorized, these results were combined with the evergreen and deciduous pixels from the original classification. Finally, a 3×3 majority filter was applied to eliminate "salt-and-pepper" pixels and complete the thematic map. Such post-classification filters are commonly used to remove land-cover clusters that are smaller than an analyst's minimum mapping unit of interest (Jensen, 2005).

TABLE 1. URBAN LAND-COVER CATEGORIZATION SCHEME FOR HYBRID CLASSIFICATION

Class	Land-cover Type	Description
1	Impervious	Transportation infrastructure (roads, parking lots, etc.), rooftops, recreational areas (i.e., tennis courts), and all other manmade impervious surfaces that are paved or built
2	Water	Lakes, ponds, rivers, streams, pools, and all other natural and artificial surface waters
3	Bare/Disturbed soil	Construction sites, landfills, gravel areas, or any other unpaved non-vegetated surface
4	Deciduous	Trees or shrubs that shed their leaves before the winter (mostly hardwood species).
5	Evergreen	Trees or shrubs that keep their leaves throughout the winter (mostly coniferous species)
6	Herbaceous	Urban grasses (yards, recreational fields, vegetated road medians, etc.) of varying degrees of maintenance

Point-based Thematic Accuracy Assessment

To assess the thematic accuracy of the hybrid land-cover classification using a traditional point-based technique, a reference dataset was created consisting of 300 randomly selected points. The land-cover at each point was photointerpreted using the fused QuickBird image and the land-cover classes described in Table 1. Fifty points were evaluated within each of these classes using a 3×3 pixel majority interpretation centered on the point. In general, a reference data set for accuracy assessment of any thematic map must adequately represent the scale, detail, and classification scheme of the map itself (Khorram *et al.*, 1999). This has special implications for high spatial resolution image analysis that will be discussed later in this paper. In order to assess the integrity of QuickBird photointerpretation for these particular land-cover types, a separate field-based reference dataset was generated and indicated 100 percent photointerpretation accuracy (27/27). Using the image-based reference data, classification validity was reported in terms of producer's accuracy, user's accuracy, and overall classification accuracy as well as through category and overall Kappa (κ) statistics.

Area-based Thematic Accuracy Assessment

In order to further assess the quality of this land-cover product, land-cover was digitized within a random sample of 50 residential property parcels, 10 commercial parcels, and 10 five-meter buffers of road segments throughout the study area. Within each of these regions, polygons were manually delineated based on the six-category classification scheme. Features were digitized based on their appearance in the pan-sharpened QuickBird image displayed as a color-infrared composite. Any impervious feature obscured by overhanging vegetation such as tree canopy would be delineated from that vertical perspective without deference to ground-level boundaries. The minimum mapping unit (MMU) for this effort was 3×3 (0.61 m) pixels or 3.35 m^2. The digitized area totaled 9.1 ha (residential), 8.1 ha (commercial), and 1.1 ha (road buffer), with a linear total of 970 road-segment meters digitized. Foody (2002), in tracing the history of thematic accuracy assessment, states that area-based accuracy assessment has limited utility because, in reality, mapped area is correct only if it is mapped in the right place. This critique is well-founded. Accordingly, area-based accuracy assessment was intended here to supplement point-based assessment in evaluating mapping accuracy at the localized scale of individual land parcels and road buffers. Comparisons here were made using measures of Pearson's correlation between per-region percent land-cover as well as mean and standard deviation percent land-cover error (reference minus classified) for all three region types. Additionally, for imperviousness, areal estimates based on all regions within each type were aggregated and compared to summary reference area figures.

Land-cover Map and Conventional Accuracy Assessment Results

Table 2 presents the error matrix for the initial hybrid classification. The overall accuracy of this classification was 83.0 percent and the κ statistic was 0.796. Within the six-category scheme, producer's accuracies ranged from 69.1 percent to 97.6 percent, while user's accuracies ranged from 66.0 percent to 94.0 percent. All category κ statistics were between 0.61 and 0.92. For four of the categories in this six-category scheme, user's and producer's accuracy were both above 75 percent, and κ was above 0.75.

Two accuracy metrics in this matrix demonstrating the greatest areas of classification confusion were herbaceous user's accuracy and impervious producer's accuracy. With respect to the 34 percent herbaceous commission error, confusion was found with all other categories although commission of deciduous cover to herbaceous was the most pronounced. With respect to the impervious category, a producer's accuracy of 69.1 percent and user's accuracy of 94.0 percent was achieved. The two areas of greatest confusion for the impervious category were the water and herbaceous categories, with omission errors of 11.8 percent and 10.3 percent, respectively, as part of a total percent omission error of 30.8 percent.

Of this confusion, it was evident that, while omission of impervious pixels with respect to the herbaceous category had no readily available resolution, the erroneous assignment of impervious pixels to the water category had a promising GIS-based method of minimization. This was a simple image segmentation based on a GIS overlay of the lakes features and subsequent unsupervised classification within the lake-subset portion of this image. During the unsupervised phase of the initial hybrid classification, no probability weighting was used for assigning pixel clusters to either the impervious or water categories despite the *a priori* knowledge that there was comparatively little water in the study area. In this GIS-based classification refinement step, the "water" unsupervised cluster from the initial Table 2 land-cover map was re-evaluated using an additional 25-class unsupervised classification of this image subset. In this pixel re-assignment process, heavy *a priori* weight was given to the impervious category. The output from this stage was then integrated into the initial land-cover map, forming an intermediate land-cover map. Next, in the 25-cluster output from the separate lake-subset unsupervised classification, heavy *a priori* weight was given to water in assigning pixels to one of the six land-cover categories. When this image was combined with the initial thematic map, its "water" pixels supplanted intermediate land-cover map pixels where this assignment was not already made, resulting in the final land-cover map.

The thematic accuracy of this final land-cover map was assessed using the same methods described for use with the initial map. The resulting error matrix is presented in Table 3. Pairwise comparison of error matrices based on the Z-test of

TABLE 2. ERROR MATRIX FOR INITIAL LAND-COVER MAP (OVERALL κ STATISTICS = 0.796, σ = 0.0265, AND 0.95 CI: 0.7441 to 0.8479)

Category	1	2	3	4	5	6	Row Total	User's Accuracy (%)	Kappa (κ)
1. Impervious	**47**	0	2	0	1	0	50	94.0	0.92
2. Water	8	**40**	0	0	0	2	50	80.0	0.77
3. Bare/disturbed	7	0	**41**	0	0	2	50	82.0	0.79
4. Deciduous	0	0	0	**44**	5	1	50	88.0	0.85
5. Evergreen	2	0	0	4	**44**	0	50	88.0	0.85
6. Herbaceous	4	1	2	8	2	**33**	50	66.0	0.61
Column Total	68	41	45	56	52	38	300		
Producer's Accuracy (%)	69.1	97.6	91.1	78.6	84.6	86.8		**83.0**	

TABLE 3. ERROR MATRIX FOR FINAL LAND-COVER MAP AFTER GIS-BASED REFINEMENT (OVERALL κ STATISTICS = 0.872, σ = 0.0224, AND 0.95 CI: 0.8282 to 0.9158)

Category	1	2	3	4	5	6	Row Total	User's Accuracy (%)	Kappa (κ)
1. Impervious	**45**	0	4	0	0	1	50	90.0	0.88
2. Water	0	**50**	0	0	0	0	50	100	1.00
3. Bare/disturbed	4	0	**45**	0	0	1	50	90.0	0.88
4. Deciduous	0	0	0	**46**	2	2	50	92.0	0.90
5. Evergreen	0	0	0	5	**44**	1	50	88.0	0.86
6. Herbaceous	6	0	0	3	3	**38**	50	76.0	0.72
Column Total	55	50	49	54	49	43	300		
Producer's Accuracy (%)	81.8	100	91.8	84.9	89.8	88.4		**89.3**	

κ values (Congalton and Green, 1999) showed that the initial (Table 2) and final accuracy (Table 3) matrices were significantly different (Z = 2.190274491, at 95 percent confidence level) and there was a significant improvement from the initial classification. Relative to the initial map, measures of overall accuracy and κ statistic were improved to 89.3 percent and 0.87, respectively. Producer's accuracy for the impervious category, 69.1 percent, was improved to 80.4 percent; this increase reflects the elimination of impervious confusion with water, a category classified perfectly according to this assessment, in which user's and producer's accuracies were both 100 percent and κ was 1.0. Numeric improvements in impervious producer's accuracy and water user's accuracy were the only category accuracy changes that exceeded the standard error of the corresponding accuracies in the initial land-cover map assessment. This statistical difference reinforced qualitative findings of this impervious/water refinement. Overall, all categories in the final land-cover map exhibited user's and producer's accuracies greater than 75 percent and κ statistics greater than 0.70. According to this final land-cover map, the study area is primarily composed of herbaceous cover (33.6 percent), followed by approximately equal amounts of impervious and deciduous cover (23.6 percent each) and a smaller extent of evergreen vegetation (14.2 percent), bare/disturbed soil (4.2 percent), and water (0.8 percent).

Area-based Accuracy Assessment Results

Table 4 presents the results of area-based accuracy assessment within the random sample of residential and commercial parcels and the road-segment buffers. Pearson's correlation coefficients between classified and digitized percent land-cover were at least 0.80 for all land-cover categories in all digitized regions. For the impervious category, all correlation coefficients were at least 0.90. The highest correlation coefficient for any category was 0.997 with respect to impervious surface percentage within the commercial parcels. As evidenced by the mean percent error (classified minus digitized percent land-cover, per sample), classified

TABLE 4. AGREEMENT BETWEEN CLASSIFIED AND DIGITIZED PERCENT LAND-COVER VALUES WITHIN SAMPLED LAND-USE REGIONS BY REGION TYPE

		Residential	Commercial	Road Segments
Land-cover Category	Statistic	Samples = 50 Total area = 21.7 ac	10 19.9 ac	10 2.6 ac
Impervious	Percent error, mean	−6.9	−2.1	−7.9
	Percent error, standard deviation	5.7	2.0	6.9
	Pearson's coefficient of correlation	0.905	0.997	0.942
Water	Percent error, mean	−0.1	0.0	0.0
	Percent error, standard deviation	0.7	0.0	0.0
	Pearson's coefficient of correlation	0.980	—*	—*
Bare/Disturbed	Percent error, mean	0.2	0.0	0.8
	Percent error, standard deviation	0.8	0.5	4.3
	Pearson's coefficient of correlation	0.099**	0.963	−0.099**
Deciduous	Percent error, mean	−4.3	−5.0	−0.9
	Percent error, standard deviation	8.1	6.1	2.2
	Pearson's coefficient of correlation	0.912	0.991	0.833
Evergreen	Percent error, mean	−1.0	1.1	−0.4
	Percent error, standard deviation	7.2	2.6	2.1
	Pearson's coefficient of correlation	0.928	0.993	0.973
Herbaceous	Percent error, mean	12.1	6.1	8.5
	Percent error, standard deviation	8.0	4.0	7.1
	Pearson's coefficient of correlation	0.885	0.938	0.932

*indicates result was not meaningful due to division by zero
**indicates result was heavily impacted by predominantly "zero percent" land-cover values

impervious percentage estimates were generally lower than reference percentages, but only by an average error across all region types of 5.6 percent. By contrast, classified herbaceous percentage estimates were generally higher than reference percentages, again by a small across-region type average of 8.9 percent. The herbaceous class, incidentally, also evidenced the highest mean percent error for any category, 12.1 percent within the residential parcels.

Aggregate estimates of impervious surface area from the classification within digitized regions are presented in Table 5. For all three region types, impervious surface area was underestimated, a function of the consistently low per-region percent estimates. For the commercial parcels and road segments, however, this error was less than 10.0 percent. The high accuracy in these regions (96.9 percent and 92.4 percent, respectively) is contrasted by that within the residential parcels (63.0 percent). This latter figure is distinctly lower than the two former, despite similar mean percent impervious error values, because impervious surfaces were much more extensive in commercial parcels (mean coverage, 74 percent) and road segments (mean coverage, 84 percent) than in residential parcels (mean coverage, 22 percent). Thus, the same mean percent error for this land-cover type represented a proportionally larger accounting deficiency overall for residential parcels.

Discussion

The land-cover maps produced by the hybrid per-pixel classification employed in this study illustrate some, but not all, of the complications purported to plague traditional approaches to high spatial resolution image classification. There were three vegetation categories and three non-vegetation categories in the six-category land-cover scheme used here. In general, classification error in the final land-cover map was partitioned by these two groupings. Within the deciduous category, for example, confusion only existed with other vegetated cover types. This is the type of error that suggests that, despite its high spatial and radiometric resolution, the limited spectral content of QuickBird imagery was an obstacle to per-pixel classification. It was qualitatively apparent, however, that there were significant textural differences between, for example, the appearance in this imagery of forested and herbaceous vegetation. Just as Chubey *et al.* (2006) used texture metrics successfully in a high spatial resolution imagery-based forest classification within an undeveloped landscape, this approach could be a partial answer to spectral overlap in urban vegetation studies.

Spectral overlap was also a factor limiting discrimination between impervious surfaces and bare/disturbed soil cover types. These categories were confused in 9.0 percent and 8.0 percent of respective reference data in the initial and final land-cover maps. These two land-cover types both have diverse representations in urban landscapes, and bare or disturbed soil in urban watersheds can have ecological implications paramount to those of impervious surface coverage (Singh *et al.*, 2003; Faucette *et al.*, 2005; Hayes *et al.*, 2005). Herold *et al.* (2003) catalogued urban reflectance and found that bare soil was confused with asphalt surfaces because neither surface type has distinct absorption features. Compounding this spectral overlap, the irregular shape of disturbed soil regions may mean that object-oriented analyses will also struggle to distinguish this cover type from developed surfaces. Bare or disturbed surfaces, though, are generally not extensive in urban landscapes except in extremely arid regions, and their extent can perhaps be manually delineated without undue burden. This was the approach of Cablk and Minor (2003) in their Ikonos-based morphological analysis of urban impervious surface. If this is not suitable for a particular urban application, it may be useful for analysts to further borrow soil reflectance knowledge from agricultural remote sensing, such as that of moisture content analyses (Alvarez-Mozos *et al.*, 2005).

TABLE 5. AREA-BASED PRODUCER'S ACCURACY OF IMPERVIOUS SURFACE MAPPING BY LAND-USE REGION TYPE

Region Type	Classification area, m^2	Reference area, m^2	Difference, m^2	Percent Accuracy
Residential	9,674	15,354	−5,680	63.0
Commercial	86,107	88,862	−2,755	96.9
Road segments	8,146	8,819	−673	92.4

It was expected that shadows would compound spectral overlap among several land-cover types, and that this complication would severely limit per-pixel classification. This expectation was not encountered here. Confusion among vegetated feature types, the reflectance of which is inherently heterogeneous, was exacerbated by shadowing. Additionally, accurate classification within herbaceous and impervious surfaces was also substantially prevented in areas adjacent to tree coverage due to shadows. Nonetheless, shadows were not considered an overall classification issue because they did not constitute a proportionally extensive part of the particular QuickBird image used here. Shadows were minimized by the mid-afternoon, summer time of collection, plus the similarity between the sun's elevation and azimuth and those of the satellite. These variables should be of high concern to analysts interested in purchasing high spatial resolution satellite imagery. Quantitatively, only 2 of the 15 errors associated with impervious surface in the final land-cover map were definitively due to the presence of shadows: one impervious reference point classified as herbaceous and one herbaceous reference point classified as impervious.

As seen in the accuracy analysis for the initial land-cover map, spectral overlap was a problem between water and impervious surface, although not because of shadows. Simple integration of ancillary GIS data minimized the effect of this problem. In the final land-cover map, the water category was perfectly classified. The substantial commission of impervious reference points to water in the first land-cover classification was essentially eliminated in this second output. Furthermore, this successful classification did not appreciably degrade the initial success of impervious surface accounting. While this particular application of GIS data integration was specific to a distinct confusion area and depended heavily on suitable data co-registration, it demanded only basic *a priori* knowledge of water features that is likely to be true of many potential urban study areas.

The initially counterintuitive finding of commission of impervious reference points to the herbaceous category was explained by a simple examination of those erroneous points. This confusion represented the greatest single source of error in the final land-cover map. Of the six impervious reference points incorrectly classified as herbaceous, all six were located along boundary lines between herbaceous and impervious features. Such boundary lines are common in urban watersheds, as they are found along roads, driveways, parking lots, and buildings. Indeed, these transitions make up much of the patchwork that is the urban landscape. Even in high spatial resolution imagery, such contrasts are delineated by historically problematic "mixed pixels" (Foody, 1997), and these pixels posed classification difficulties as they have in other high spatial resolution studies (Segl *et al.*, 2003).

The "edge pixel" problem is central to understanding the results of the area-based analysis of error (Figure 3) of the study's final land-cover map. Overall, the level of accuracy determined here suggests that per-pixel classification is capable of mapping urban land-cover at high levels of detail. As mentioned above, Pearson's correlation coefficients (when available) were at least 0.80 for all land-cover categories for each type of region (residential, commercial, and transportation). This high level of agreement between classified and reference land-cover percentages is a notable achievement for per-pixel classification. In the commercial parcels, this correlation was determined to be nearly perfect for impervious surface percentage. Total area imperviousness calculations from classified and reference outputs matched to a substantial extent for each land-use type, although this match was markedly better in commercial and transportation (97 percent and 92 percent match, respectively) regions than for residential regions (63 percent match).

Taken as a whole, however, these results are very informative as to the limiting effect of "edge pixels" on per-pixel, high spatial resolution image classification. The accuracy data indicate that, while, impervious features were mapped here with moderate success, linear boundaries were not mapped very accurately, and discrete image objects, such as buildings and roads, were not depicted in the final land-cover map with much real-world geometry. These conclusions are drawn on the basis of the significant impervious/herbaceous "edge pixel" error as well as the consistent under-estimation of imperviousness and over-estimation of herbaceous cover in all three types of digitized land-use regions. In commercial and roads areas, where area-based impervious accuracy was high, the ratio of real-world imperviousness to vegetated features was also high. In residential areas, where vegetated features and their boundaries with impervious features were extensive, area-based impervious accuracy was low. In addition, houses and driveways in residential parcels were frequently and considerably obscured by overhanging tree canopy.

In sum, the highly heterogeneous nature of residential parcel land-cover was a challenge for the per-pixel classification methods used here. Much of this heterogeneity was expressed in the form of "edge pixels," and, as mapped, real-world impervious geometry was eroded in company with falsely expanded vegetated cover. In contrast to the classification methods used here, the goal behind object-oriented classification is to isolate image objects, not pixels. Thus, land-cover shape is not just preserved in a successful object-oriented classification but is, in fact, a primary basis for such classification. The advantage of such an approach is empirically suggested by the "edge pixel" complications reported here. In this urban study area, however, per-pixel classification was wholly effective wherever vegetated/non-vegetated boundaries were less extensive, such as in commercial areas. The predominance of impervious surfaces in these land uses, as well as their size, makes them important inputs for environmental modeling efforts (Butcher, 1999; Gillies *et al.*, 2003)

The "edge pixel" limitation of this land-cover map was significant but not fully characterized by traditional point-based accuracy assessment. One reason for this is that, in generating the reference dataset for this traditional accuracy assessment, mixed pixels were a challenge to interpret, although this concern is not new to the development of thematic map reference data (Khorram, 1999). For high spatial resolution data, field-generated data may be especially appropriate despite the difficulties its acquisition often poses (Cablk and Minor, 2003). In general, the heterogeneous nature in which features are represented by high spatial resolution imagery may not be adequately tested by conventional accuracy methods. Barr and Barnsley (2000) discussed this problem and addressed it in their study by examining morphological accuracy, the goal of which was to evaluate the accuracy of land-cover shape, as well as total area-mapping results. Previously, it has been noted that a limitation of the traditional error matrix is that it does not describe the spatial distribution of classification error (Morisette *et al.*, 1999). This may have unique implications for the detail that is sought through high spatial resolution image classification.

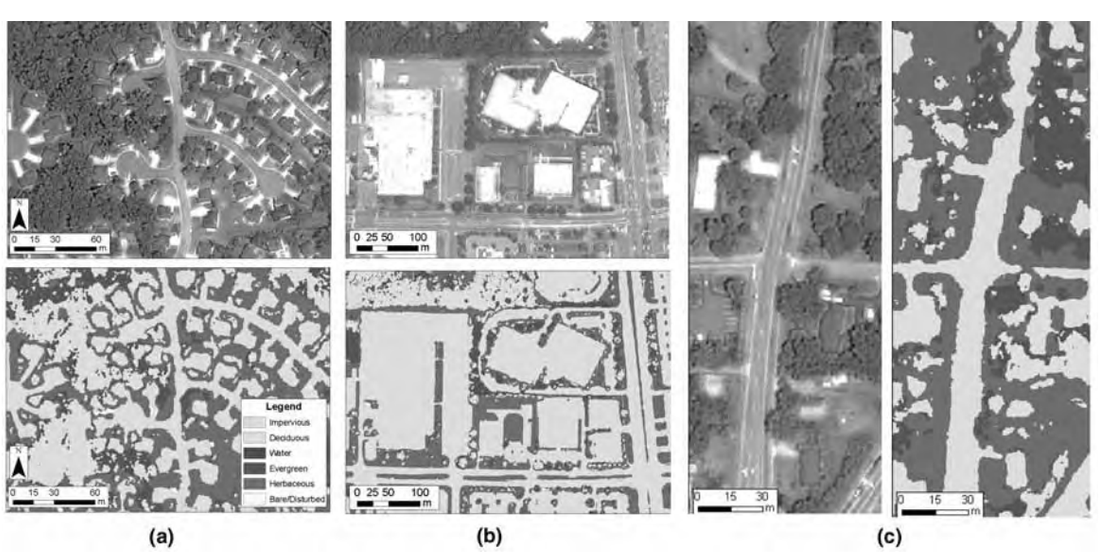

Figure 3. Land-cover mapping results within selected (a) residential, (b) commercial, and (c) road-corridor regions and corresponding true-color QuickBird imagery. A color version of this figure is available at the ASPRS website: **www.asprs.org**.

Conclusions

This paper has examined the use of conventional per-pixel image classifiers, the maximum likelihood and ISODATA algorithms, in developing an urban land-cover map using pan-sharpened 0.61 m QuickBird imagery. An exclusively spectral-based classification approach, coupled with a simple GIS masking step, was used to generate a six-category land-cover map with 89.3 percent overall accuracy. Impervious surfaces were mapped particularly well ($\kappa = 0.88$). Total impervious surface estimates matched reference figures with 96.9 percent and 92.4 percent agreement in commercial and road buffer reference regions. Area-based imperviousness accuracy estimates reinforced qualitative findings, however, that real-world geometry was not well-represented among certain land-use types. In highly heterogeneous residential areas, for example, the misrepresentation of linear boundaries between impervious surfaces and vegetated cover types was pronounced.

An ancillary GIS layer depicting study area lakes was used to virtually eliminate an initial area of confusion between impervious surfaces and water. Such ready integration of GIS data is inherent advantage to the analysis of high spatial resolution imagery. A solution to another classification problem, the lack of discriminatory power among vegetated cover types, was not so readily apparent. Importantly, though, none of the classification difficulties reported here was extensively due to the effects of shadows, as had been expected. In fact, confusion was more commonly due to image heterogeneity and reflectance overlap among illuminated versions of different cover types. Analysts are encouraged to carefully consider high spatial resolution image acquisition parameters to minimize the potential effects of shadowing.

Future work should continue to investigate the use of familiar spectral-based approaches to mapping high spatial resolution imagery, and the results of this study indicate that, for mapping particular urban land-cover types, these approaches can be highly efficient and accurate. In this study, impervious surface mapping accuracy was higher in areas where reference data indicated that it was more extensive and continuous, such as in commercial parcels. The distribution and shape of such cover types in heterogeneous areas may be more accurately mapped by emerging object-oriented approaches customized to exploit detailed object morphology. Traditional spectral-based approaches, however, are comparatively simple and well-documented. In this light, the results of this study suggest that existing per-pixel classification methods present an efficient, widely available, and familiar means of land-cover map derivation for particular applications of this exciting new data source.

Acknowledgments

This study was enabled through funding provided by the North Carolina Water Resources Research Institute (NC WRRI) for the project "Integration of High Resolution Imagery in Cost-Effective Assessment of Land Use Practices Influencing Erosion and Sediment Yield (2004–2006)." Ancillary data was acquired from the Wake County and City of Raleigh GIS iMaps server.

References

Al-Khudhairy, D.H.A., I. Caravaggi, and S. Glada, 2005. Structural damage assessments from Ikonos data using change detection, object-oriented segmentation, and classification techniques, *Photogrammetric Engineering & Remote Sensing*, 71(8):825–837.

Alvarez-Mozos, J., J. Casali, M. Gonzalez-Audicana, and N.E.C. Verhoest, 2005. Correlation between ground measured soil moisture and RADARSAT-1 derived backscattering coefficient over an agricultural catchment of Navarre (North of Spain), *Biosystems Engineering*, 92:119–133.

Barr, S., and M. Barnsley, 2000. Reducing structural clutter in land cover classifications of high spatial resolution remotely-sensed images for urban land use mapping, *Computers and Geosciences*, 26:433–449.

Burkholder, J.M., E.J. Noga, C.H. Hobbs, and H.B. Glasgow, 1992. New phantom dinoflagellate is the causative agent of major estuarine fish kills, *Nature*, 358:407–410.

Butcher, J.B., 1999. Forecasting future land use for watershed assessment, *Journal of the American Water Resources Association*, 35:555–565.

Cablk, M.E., and T.B. Minor, 2003. Detecting and discriminating impervious cover with high-resolution Ikonos data using principal component analysis and morphological operators, *International Journal of Remote Sensing*, 24:4627–4645.

Cakir, H.I., and S. Khorram, 2004. *Methods, Systems and Computer Program Products for Fusion of High Spatial Resolution Imagery with Low-spatial but High-spectral Resolution Imagery Using Correspondence Analysis*, November 04, U.S. Patent Application No: 10/982,054.

Carleer, A.P., O. Debeir, and E. Wolff, 2005. Assessment of very high spatial resolution satellite image segmentations, *Photogrammetric Engineering & Remote Sensing*, 71(11):1285–1294.

Cheng, H.D., X.H. Jiang, Y. Sun, and J.L. Wang, 2001. Color image segmentation: Advances and prospects, *Pattern Recognition*, 34:2259–2281.

Chubey, M.S., S.E. Franklin, and M.A. Wulder, 2006. Object-based analysis of Ikonos-2 imagery for extraction of forest inventory parameters, *Photogrammetric Engineering & Remote Sensing*, 72(3):383–394.

Clark, D.B., C.S. Castro, L.D.A. Alvarado, and J.M. Read, 2004. Quantifying mortality of tropical rain forest trees using high-spatial-resolution satellite data, *Ecology Letters*, 7:52–59.

Congalton, R.G., K. Birch, R. Jones, and J. Schriever, 2002. Evaluating remotely sensed techniques for mapping riparian vegetation, *Computers and Electronics in Agriculture*, 37:113–126.

Congalton, R.G., and K. Green, 1999. *Assessing the Accuracy of Remotely Sensed Data: Principles and Practices*, Lewis Publishers, Boca Raton, Florida, 137 p.

Dare, P.M., 2005. Shadow analysis in high-resolution satellite imagery of urban areas, *Photogrammetric Engineering & Remote Sensing*, 71(1):169–177.

Faucette, L.B., C.F. Jordan, L.M. Risse, M. Cabrera, D.C. Coleman, and L.T. West, 2005. Evaluation of stormwater from compost and conventional erosion control practices in construction activities, *Journal of Soil and Water Conservation*, 60:288–297.

Fisher, J., and S. Goetz, 2001. Considerations in the use of high spatial resolution imagery: An applications research assessment, *Proceedings of the ASPRS 2001 Annual Convention*, 23–27 April, St. Louis, Missouri, unpaginated CD-ROM.

Foody, G.M., 1995. Land-cover classification by an artificial neural-network with ancillary information, *International Journal of Geographical Information Systems*, 9:527–542.

Foody, G.M., 1997. Fully fuzzy supervised classification of land cover from remotely sensed imagery with an artificial neural network, *Neural Computing and Applications*, 5:238–247.

Foody, G.M., 2002. Status of land cover classification accuracy assessment, *Remote Sensing of Environment*, 80:185–201.

Gao, J., H.F. Chen, Y. Zhang, and Y. Zha, 2004. Knowledge-based approaches to accurate mapping of mangroves from satellite data, *Photogrammetric Engineering & Remote Sensing*, 70(12):1241–1248.

Gillies, R.R., J.B. Box, J. Symanzik, and E.J. Rodemaker, 2003. Effects of urbanization on the aquatic fauna of the Line Creek watershed, Atlanta – A satellite perspective, *Remote Sensing of Environment*, 86:411–422.

Goetz, S., R. Wright, A. Smith, E. Zinecker, and E. Schaub, 2003. Ikonos imagery for resource management: Tree cover, impervious surfaces, and riparian buffer analyses in the mid-Atlantic region, *Remote Sensing of Environment*, 88:195–208.

Hayes, S.A., R.A. McLaughlin, and D.L. Osmond, 2005. Polyacrylamide use for erosion and turbidity control on construction sites, *Journal of Soil and Water Conservation*, 60:193–199.

Herold, M., M.E. Gardner, and D.A. Roberts, 2003. Spectral resolution requirements for mapping urban areas, *IEEE Transactions on Geoscience and Remote Sensing*, 41:1907–1919.

Herold, M., X.H. Liu, and K.C. Clarke, 2003. Spatial metrics and image texture for mapping urban land-use, *Photogrammetric Engineering & Remote Sensing*, 69(9):991–1001.

Hu, X.Y., C.V. Tao, and B. Prenzel, 2005. Automatic segmentation of high-resolution satellite imagery by integrating texture, intensity, and color features, *Photogrammetric Engineering & Remote Sensing*, 71(12):1399–1406.

Jennings, D., S. Jarnagin, and D. Ebert, 2004. A modeling approach for estimating watershed impervious surface area from national land-cover data 92, *Photogrammetric Engineering & Remote Sensing*, 70(11):1295–1307.

Jensen, J., 2005. *Introductory Digital Image Processing: A Remote Sensing Perspective*, Second edition, Prentice Hall, Upper Saddle River, New Jersey.

Jensen, J.R., and D.C. Cowen, 1999. Remote sensing of urban suburban infrastructure and socio-economic attributes, *Photogrammetric Engineering & Remote Sensing*, 65(6):611–622.

Kelly, M., D. Shaari, Q.H. Guo, and D.S. Liu, 2004. A comparison of standard and hybrid classifier methods for mapping hardwood mortality in areas affected by "sudden oak death," *Photogrammetric Engineering & Remote Sensing*, 70(11):1229–1239.

Khorram, S., G.S. Biging, N.R. Chrisman, D.R. Colby, R.G. Congalton, J.E. Dobson, R.L. Ferguson, M.F. Goodchild, J.R. Jensen, and T.H. Mace, 1999. *Accuracy Assessment of Remote Sensing-Derived Change Detection*, Monograph, American Society for Photogrammetry and Remote Sensing.

King, R.S., M.E. Baker, D.F. Whigham, D.E. Weller, T.E. Jordan, P.F. Kazyak, and M.K. Hurd, 2005. Spatial considerations for linking watershed land cover to ecological indicators in streams, *Ecological Applications*, 15:137–153.

Ludwig, R., M. Probeck, and W. Mauser, 2003. Mesoscale water balance modelling in the Upper Danube watershed using subscale land cover information derived from NOAA-AVHRR imagery and GIS-techniques, *Physics and Chemistry of the Earth*, 28:1351–1364.

Lunetta, R.S., J. Ediriwickrema, J. Iiames, D.M. Johnson, J.G. Lyon, A. McKerrow, and A. Pilant, 2003. A quantitative assessment of a combined spectral and GIS rule-based land-cover classification in the Neuse River Basin of North Carolina, *Photogrammetric Engineering & Remote Sensing*, 69(2):299–310.

Maeder, J., S. Narumalani, D.C. Rundquist, R.L. Perk, J. Schalles, K. Hutchins, and J. Keck, 2002. Classifying and mapping general coral-reef structure using Ikonos data, *Photogrammetric Engineering & Remote Sensing*, 68(12):1297–1305.

McMahon, G., and O. Lloyd, 1995. *Water Quality Assessment of the Albemarle-Pamlico Drainage Basin, North Carolina and Virginia: Environmental Setting and Water-Quality Issues*, U.S. Geological Survey Open File Report 95–136, U.S. Geological Survey, Raleigh, North Carolina, 72 p.

Miura, H., and S. Midorikawa, 2006. Updating GIS building inventory data using high-resolution satellite images for earthquake damage assessment: Application to metro Manila, Philippines, *Earthquake Spectra*, 22:151–168.

Morisette, J.T., S. Khorram, and T. Mace, 1999. Land-cover change detection enhanced with generalized linear models, *International Journal of Remote Sensing*, 20:2703–2721.

North Carolina Division of Water Quality, 2004. *North Carolina 303 (d) Impaired Waters List*, URL: *http://h2o.enr.state.nc.us/tmdl/General_303d.htm* (last date accessed: 09 January 2008).

Paerl, H.W., J.L. Pinckney, J.M. Fear, and B.L. Peierls, 1998. Ecosystem responses to internal and watershed organic matter loading: Consequences for hypoxia in the eutrophying Neuse river estuary, North Carolina, USA, *Marine Ecology-Progress Series*, 166:17–25.

Pohl, C., and J.L. van Genderen, 1998. Multisensor image fusion in remote sensing: Concepts, methods and applications, *International Journal of Remote Sensing*, 19:823–854.

Sawaya, K., L. Olmanson, N. Heinert, P. Brezonik, and M. Bauer, 2003. Extending satellite remote sensing to local scales: Land and water resource monitoring using high-resolution imagery, *Remote Sensing of Environment*, 88:144–156.

Segl, K., S. Roessner, U. Heiden, and H. Kaufmann, 2003. Fusion of spectral and shape features for identification of urban surface cover types using reflective and thermal hyperspectral data, *ISPRS Journal of Photogrammetry and Remote Sensing*, 58:99–112.

Singh, V., T. Piechota, and D. James, 2003. Hydrologic impacts of disturbed lands treated with dust suppressants, *Journal of Hydrologic Engineering*, 8:278–286.

Song, M., D.L. Civco, and J.D. Hurd, 2005. A competitive pixel-object approach for land cover classification, *International Journal of Remote Sensing*, 26:4981–4997.

Svab, A., and K. Osti, 2006. High-resolution image fusion: Methods to preserve spectral and spatial resolution, *Photogrammetric Engineering & Remote Sensing*, 72(5):565–572.

Thomas, N., C. Hendrix, and R. Congalton, 2003. A comparison of urban mapping methods using high-resolution digital imagery, *Photogrammetric Engineering & Remote Sensing*, 69(9):963–972.

U. S. Census Bureau, 2006. Population Estimates for the 100 U.S. Counties with the Largest Numerical Increase from April 1, 2000 to July 1, 2005 U. S. Department of Commerce, Washington, D.C., URL: *http://www.census.gov/Press-Release/www/2006/countypop05-table5.pdf* (last date accessed: 09 January 2008).

Walsh, C.J., T.D. Fletcher, and A.R. Ladson, 2005. Stream restoration in urban catchments through redesigning stormwater systems: Looking to the catchment to save the stream, *Journal of the North American Benthological Society*, 24:690–705.

Wang, L.Z., J. Lyons, and P. Kanehl, 2001. Impacts of urbanization on stream habitat and fish across multiple spatial scales, *Environmental Management*, 28:255–266.

Warner, T.A., and K. Steinmaus, 2005. Spatial classification of orchards and vineyards with high spatial resolution panchromatic imagery, *Photogrammetric Engineering & Remote Sensing*, 71(1):179–187.

Williams, E.S., and W.R. Wise, 2006. Hydrologic impacts of alternative approaches to storm water management and land development, *Journal of the American Water Resources Association*, 42:443–455.

Yang, L., G. Xian, J. Klaver, and B. Deal, 2003. Urban land-cover change detection through sub-pixel imperviousness mapping using remotely sensed data, *Photogrammetric Engineering & Remote Sensing*, 69(10):1003–1010.

(Received 19 December 2006; accepted 07 August 2007; revised 23 October 2007)